MULTI-FRACTION SEDIMENT TRANSPORT MODELLING IN MIKE 3 FM

Maycon Fontana[1], Athanasios Petridis[2], and Kasper Kærgaard[3]

The present study investigates the experimental results of the MUSA project flume laboratory experiments concerning phase 1D of the scope of work. It aims to represent the laboratory conditions through a numerical flume established in MIKE Powered by DHI software. Additionally, a new approach to combining the sand-gravel model with the mud transport model is tested. The model predictions of suspended sediment concentration are within a factor of 2 to 5 for both the sand and mud fractions when compared to the laboratory measurements. Thus, the new combined mud and sand-gravel transport model is deemed able to represent the dynamics of the sand and fines fractions in a sand-mud mixed bed under combined waves and currents action.

Keywords: multi-fraction sediment transport; numerical flume; MIKE 3 FM

INTRODUCTION

Estuaries and tidal basins play an important role both in terms of ecosystem services and human activities (e.g. navigation). In this sense, predicting and understanding the dynamics and composition of the sea bed is crucial. The bed composition of estuaries and tidal basins consists of mixtures of mud and sand. The hydrodynamics conditions associated with wave action in such environments lead to a complex interaction between sand and mud. However, the current numerical modelling often treats the sediment fractions according to a decoupled approach. This is partly due to the limited knowledge regarding the behavior of sand-mud interaction.

In this sense, DHI is currently developing a new multi-fraction sediment transport model to be implemented in MIKE 3 FM. The main goal is a combined Mud – Sand – Gravel transport model for combined waves and currents (i.e. estuaries). The new model implementation has been carried out in part as part of the MUSA project which is further described in following sections.

This paper compares the experimental results of the MUSA project flume laboratory experiments with predictions from a digital flume established using MIKE 3 FM and a newly developed sediment transport formulation. It investigates the experiments concerning phase 1D of the MUSA scope of work.

In general, phase 1D of the MUSA project addressed assessing the erodibility, sediment concentration, and sediment transport of mud-sand mixtures under combinations of waves and currents in a long wave flume.

The numerical flume is basically a copy of the laboratory flume. The model is built in the MIKE 3 Flow Model FM. The hydrodynamics module (HD) simulates the hydrodynamics, and the mud transport module (MT) calculates the sediment dynamics in the flume. The utilized MT module in this investigation corresponds to a new framework, in each the sand fraction is modelled following (Wu, Wang and JIA 2000), (Wu and Lin 2014), and (Wu and Lin 2014) – Wu framework. The mud fraction is calculated following the existing MT module with specific improvements. The simulated hydrodynamics and sediment fractions are compared to the laboratory measurements and the results are assessed.

FLUME EXPERIMENTS

MUSA project

The MUSA research project aims to enhance the understanding of the dynamics of sand-mud mixtures - the project is detailed described in (Lenssinck and Ton 2024). The scope is conducted by a consortium of contractors, consultants, and research organizations through the following activities:

- Literature analysis.
- Laboratory experiments.
- Field measurements.
- Development and improvement of formulations on sand-mud dynamics.
- Development of engineering tools.
- Implementation of formulations in numerical software.

During the four-year working period (2020-2023), the MUSA team has delivered various reports covering these intermediated activities such as literature analysis, laboratory experiments, and field

[1] mamf@dhigroup.com; DHI Denmark - Agern Alle 5, 2970 Hørsholm
[2] atpe@dhigroup.com; DHI Denmark - Agern Alle 5, 2970 Hørsholm
[3] kak@dhigroup.com; DHI Denmark - Agern Alle 5, 2970 Hørsholm

measurements. A synthesis report has been written which includes the essence of the new DHI multi-fraction sediment transport model.

Current-wave flume

The experiments were performed in a wave-current flume with a length of 13 m, a width of 0.4 m, and a water depth of 0.25 m. The flume warm-up period is 15 minutes, while the entire measurement cycle for one hydrodynamic condition took 45-60 minutes. The prepared sediment samples (Table 2) were placed near the centre of the flume. The sediment layer presents a total thickness in the order of 5-7cm. The measured parameters utilized in the present study are flow velocity, wave height, suspended concentration of sand (> 63 μm) and fines (< 63 μm). Table 1 presents the hydrodynamics and wave conditions for the laboratory experiments.

Table 1. Laboratory experiments: hydrodynamics and wave conditions.

Run	Depth-averaged current velocity (CS) [m/s]	Wave height (H) [m]	Wave period (T) [s]	Adjusted wave height (H_{adj}) [m]
J3	0.20	0.08	1.30	0.10
J4	0.20	0.12	1.00	0.12
J5	0.35	0.08	1.20	0.11
J6	0.75	0.06	1.00	0.12
I3	0.20	0.08	1.50	0.09
I4	0.20	0.12	1.10	0.10
I5	0.35	0.08	1.10	0.12
I6	0.75	0.06	1.00	0.12
K4	0.20	0.12	1.00	0.10
K5	0.35	0.08	1.40	0.10
K6	0.75	0.06	1.00	0.12

The experiments assess different mud and sand bed compositions (Table 2). The mixed samples combine dark grey-black mud from the harbour of Noordpolderzijl – Netherlands (NPZ) and commercial fine sand (d_{50}=0.13 mm and dry density=1600 kg/m^3).

Table 2. Laboratory experiments: hydrodynamics and wave conditions.

Experiment	Bed fines content (p_{fines}<63 μm)	Mixed sample	Mud dry density [kg/m^3]
J	13%	NPZ-harbour mud 1+ fine sand	780
I	18%	NPZ-harbour mud 1+ fine sand	780
K	30%	NPZ-harbour mud 2 + fine sand	550

MODEL DESCRIPTION

MIKE 3 Flow Model FM

MIKE 3 Flow Model FM was used for modelling the laboratory flume. The Hydrodynamic Module (HD) and Mud Transport Module (MT) have been used.

MIKE 3 Flow Model FM is based on the numerical solution of the three-dimensional incompressible Reynolds-averaged Navier-Stokes equations (DHI A/S 2022). The model consists of the continuity and momentum equations, and it is closed by a turbulent closure scheme. Horizontally, it is based on an unstructured flexible mesh and uses a finite volume solution technique. Vertically, it is based on a sigma coordinate system or a combination of sigma coordinate system and a Cartesian coordinate system.

Mud Transport

The Mud Transport module is dedicated to the modelling of fine sediment transport - which is presented in detail in (DHI A/S 2021). The module describes erosion, transport, and deposition of fined-grained material < 63 μm (silt and clay) under the action of currents and waves. The mud transport model utilized in this investigation correspond to the existing MT model with specific improvements.

The MT module consists of a “water-column” and an “in-bed” module. The link between these two modules is sources/sink terms in an advection-dispersion model. These terms in the advection-dispersion

equation depend on whether the local hydrodynamics conditions cause the bed to become eroded or allow deposition to occur.

The combination of long-period waves and wind-waves is able to re-entrain or re-suspend the deposited or consolidated sediment. While the processes in the bed are described in a multi-layer bed scheme. Each layer is described by a critical shear stress for erosion, erosion coefficient, power of erosion, and erosion function.

The existing MT model describes each layer with a specific density of dry sediment. In the new MT multi-fraction model; each layer is described according to a combination of densities of dry sediment according to the modelled fractions.

The current model represents the bed as soft mud, following (Parchure and Metha 1985) formulation, since the utilized mud samples present intermediated densities. The erosion rate (E_0) and the power of erosion (α) are calibrated for each analyzed bed.

Sand Transport

The sand fraction is modelled according to a new model implementation. The approach follows the Wu framework, which introduces novel formulations to account for nonuniform sediment transport.

(Wu, Wang and JIA 2000) presents a correction factor of the critical Shields parameter related to the hiding and exposure mechanism of nonuniform sediment transport. This factor is assumed to be a function of the hiding and exposure probabilities, which are stochastically associated with the size and gradation of the bed materials. The correction factor (η_i) is calculated according to the following equations:

$$\eta_i = \left(\frac{p_{ei}}{p_{hi}}\right)^m \quad (1)$$

In which p_{ei} and p_{hi} are defined as the total exposed and hidden probabilities of particles d_i. They are calculated according to the following equations:

$$p_{ei} = \sum_{j=1}^{N} p_{bj} \frac{d_i}{d_i + d_j} \quad (2)$$

$$p_{hi} = \sum_{j=1}^{N} p_{bj} \frac{d_j}{d_i + d_j} \quad (3)$$

Where,

m: empirical parameter [-]
N: total number of particle size fractions [-]
$d_{i/j}$: sediment diameter [mm]
p_{bj}: percentage of particles *dj* in the bed material [-]

The following equation determines the critical shear stress for the incipient motion of nonuniform sediment – the hiding and exposure factor modifies the original equation suggested by (Shields 1936).

$$\theta_{ci} = \Theta_c \, \eta_i \quad (4)$$

$$\tau_{ci} = \theta_{ci} \, (\gamma_s - \gamma) d_i \quad (5)$$

Where,

τ_{ci}: critical shear stress for particle *di* [N/m^2]
Θ_c: non-dimensional critical shear stress for the corresponding mean size of the bed material (critical Shields parameter) [-]
γ_s: sediment density [kg/m^3]
γ: water density [kg/m^3]

For mud and sand mixed beds, the critical Shields parameter (or else the critical bed shear stress for erosion) is expected to be different, based on the percentage of mud content in the bed. More information, about the change of the critical Shields number in cases of sand/mud mixtures will be given in a following section.

The present implementation utilizes the RMS bed shear stresses under combined current and wave action according to (Soulsby, et al. 1993). In a current-wave flume experiment, it is believed that the approach is appropriate for estimating the actual bed shear stress during a wave cycle.

For the sand transport framework, the grain shear stress is utilized, meaning that the equivalent roughness height (k_s) used in the aforementioned formulas is given by the grain roughness (k_s=2.5d_{50}), where d_{50} is the median grain size of the sand fractions, rather than the total roughness including bed forms.

The sand transport is calculated based on the (Wu and Lin 2014) framework, utilizing the bed load formula shown below:

$$q_{bi} = p_{bi}\sqrt{(s-1)g{d_i}^3}\,0.0053\left(\frac{\tau_{RMS}}{\tau_{ci}} - 1\right)^{2.2} \quad (6)$$

The reference concentration (c_b) at the reference level (δ), shown below:

$$c_{bi} = 0.0032\frac{p_{bi}d_i}{\delta}\left(\frac{\tau_{RMS}}{\tau_{ci}} - 1\right)^{0.5} \quad (7)$$

$$\delta = max(2d_{50}, 0.5\Delta_r, 0.01h) \quad (8)$$

Where,

q_{bi}: volumetric bed load of the i^{th} fraction [m^3/s]
p_{bi}: percentage of the i^{th} fraction in the bed (active layer) [-]
s: sediment grain relative density ρ_s/ρ_w [-]
g: gravitational acceleration [m/s^2]
c_{bi}: volumetric reference concentration at the reference level for the i^{th} fraction [-]
δ: reference level [m]
Δ_r: ripple height, as measured during the experiments [m]
τ_{RMS}: wave-current RMS bed shear stress [N/m^2]

Combined mud and sand transport

For mixed sand and mud beds, the critical shear stress can be calculated using the (Wu, Perera, et al. 2017) approach. According to this approach, the critical shear stress is expected to increase for increased percentages of mud. The approach treats the bed based on three regimes: a) pure sand - low mud content (up to 5%), b) medium-high mud content and c) pure mud. In the first regime, the bed is considered to be cohesionless, even with the small addition mud, in contrast to the two other regimes, where the bed acts as cohesive. The critical shear stress for erosion in the first regime (mud content up to 5%) is described by the following equation:

$$\tau_{ceL} = \tau_{crn} + 1.25(\tau_{ce} - \tau_{crn})\min(p_m, 0.05) \quad (9)$$

Where,

τ_{ceL}: bed's critical shear stress for combined sand and mud for mixtures with low mud content (up to 5%) [N/m^2]
τ_{crn}: critical shear stress for erosion of the pure sand [N/m^2]
τ_{ce}: critical shear stress for erosion of the pure mud [N/m^2]
p_m: mud content in bed [kg/m^3]

In case the mud content increases, then the following formula can be used:

$$\tau_{cem} = \tau_{ceL} + (\tau_{ce} - \tau_{ceL})exp\left[-a\left(\frac{p_s}{p_m}\right)^{1.2}\right] \quad (10)$$

Where,

τ_{cem}: bed's critical shear stress for combined sand and mud (mud content > 5%) [N/m^2]
a: scaling coefficient [-]
p_s: sand content in bed [kg/m^3]

The critical shear stress for erosion of the pure mud case can be calculated by the following:

$$\tau_{ce} = 10.29r^{1.7} \quad (11)$$

Where, r is the solid/void volume ratio, $r = (1 - \varphi_m)/\varphi_m$ [-], with φ_m being the mud porosity. φ_m is related to the mud dry density ρ_{dm} by $\rho_{dm} = (1 - \varphi_m)\rho_s$, with ρ_s being the sediment's grain density (for quartz equal to 2650 kg/m^3).

For this study, the mud dry densities are provided for each experiment. Therefore, it becomes apparent that the dry density and critical shear stress of the pure mud case are required to calculate the bed shear stress of the sand/mud mixtures. Since these are not provided in the current study and the mud used in the different experiments is possibly not identical (NPZ mud has different dry densities, but also different percentage of fines between experiments J, I and K), the critical shear stress for erosion of the sand/mud mixture is approximated by the experiment observations. More specifically, the forcing conditions (current and waves) at incipient motion for each experiment is used to calculate the maximum combined bed shear stress and approximate the critical bed shear stress for each bed. These conditions are shown in Table 3, along with the selected critical shear stresses for each bed.

Table 3. Incipient motion conditions for experiments J, I and K, along with the selected critical bed shear stress of the sand/mud mixture (τ_{cem}).

Bed	U [m/s]	H [m]	Comment	τ_{max} [N/m^2]	Selected τ_{cem} [N/m^2]
J	0.20-0.25	0.00	Initiation of sand over dark spots	0.079 – 0.123	0.125
	0.00	0.05	Initiation of sand	0.149	
	0.00	0.06	Suspension layer=20mm	0.207	
	0.00	0.08	Mud washed out, suspension layer=30 mm, sand concentration < 10 mg/l	0.326	
I	0.20-0.25	0.00	Initiation of sand over dark spots	0.079 – 0.123	0.180
	0.00	0.05	Initiation of sand	0.149	
	0.00	0.06	Mud washed out, suspension layer=20mm	0.207	
	0.00	0.08	Mud washed out, suspension layer=30 mm, sand concentration < 10 mg/l	0.326	
K	0.25	0.00	Initiation of sand over dark spots	0.123	0.270
	0.00	0.06	Brown film of mud, no sand	0.204	
	0.00	0.08	Suspension layer=20-30 mm, sand concentration < 10 mg/l	0.326	

It has to be mentioned, that the Wu framework was not used to calculate the critical bed shear stresses, due to the absence of the pure mud dry density and its respective critical bed shear stress. In addition, the Wu framework assumes similar mud being used in the different mixtures, since they all rely on one pure mud case. However, this is possibly the case only for experiments I and K (NPZ-mud 2).

The Wu framework is however tested in the present study, keeping the aforementioned note in mind. A similar mud in all three experiments, a dry density of a theoretical pure mud case of 1500 kg/m^3 and an equivalent critical shear stress for erosion of 3.5 N/m^2 are assumed. These values are fair assumptions, based on the dry density of the mud used in the three experiments and the expected critical shear stress for erosion of such a mud. The calculated critical shear stress for erosion for experiments J (13% mud content), I (18% mud content) and J (30% mud content) are shown in Figure 1.

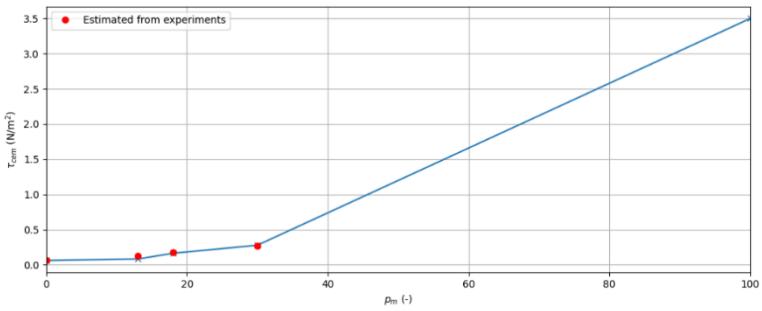

Figure 1. Critical bed shear stress as a function of mud content for the NPZ mud experiments (J, I and K).

It can be seen that the relative difference between the calculated and approximated critical shear stress of erosion for beds J (p_m=13%), I (p_m=18%) and K (p_m=30%) is -35%, -9% and +3% respectively; these are within the uncertainty for the estimated critical shear stresses based on the observations. In addition, the values calculated by the Wu framework, lie within the calculated maximum bed shear stresses for incipient motion of Table 3, namely 0.079 – 0.326 N/m^2.

Finally, the critical Shields parameter, θ_c, for the sand fraction with d_{50}=0.13 mm and ρ_s=2660 kg/m^3 is derived for each bed based on the critical bed shear stress mentioned above. The calculated values are shown in Table 4.

Table 4. Critical Shields parameter, θ_c, for the sand fraction with d_{50} grain size for experiments A, J, I and K.

Bed	θ_c
J (p_m=13%)	0.058
I (p_m=18%)	0.084
K (p_m=30%)	0.126

DIGITAL FLUME

Computational mesh

The computational mesh of the numerical model is basically a digital copy of the laboratory flume geometry. The utilized mesh is based on rectangular elements. The horizontal mesh elements present dx of 5 cm and dy of 40 cm.

Bed resistance (HD model)

The bed resistance in the hydrodynamic model follows the wave induced formulation introduced by (Fredsøe 1984). The wave forcing presented in section number is utilized for the wave contribution – no corrections are applied to the wave parameters. The roughness has been set to 0.25 x d_{50} (0.0325 mm) in all the runs - according to the sand grain size.

Recirculation scheme

The water flow is (re)circulated by a centrifugal pump with electronic control in the laboratory flume. This recirculation scheme is also represented in the digital flume by introducing a source in the upstream end of the flume and a sink in the downstream end. The suspended sediment mass located at the downstream end of the digital flume re-enters the model volume at the upstream area. The hydrodynamics condition of the specific runs is represented in the source and sink specifications. It presents a warm-up period of 15 minutes.

Wave forcing

The wave forcing has been reported in the MUSA experiments, providing the setup wave height and wave period. The waves in the flume are expected to be non-linear in some cases, requiring a higher-order scheme for estimating the wave-induces velocities over the water column. For this reason, the Isobe model is used to estimate the nearbed wave-induced velocities.

The effect of the current on the waves needs to be taken into consideration. More specifically, the existence of current affects the wave in such a way, that it behaves as it is travelling in shallower waters (kh smaller), i.e. the current smooths out the wave. Hence, the modified kh parameter is used to estimate the equivalent water depth, which then is used to calculate the nearbed wave orbital velocities with the Isobe wave model. The minimum and maximum (positive and negative half-cycle) nearbed wave orbital velocities are added on top of the measured mean velocities and are compared against the minimum and maximum measured velocities. For instance, the results of experiments I6 and K6 can be seen in Figure 2 both with and without the effect of the current on the waves.

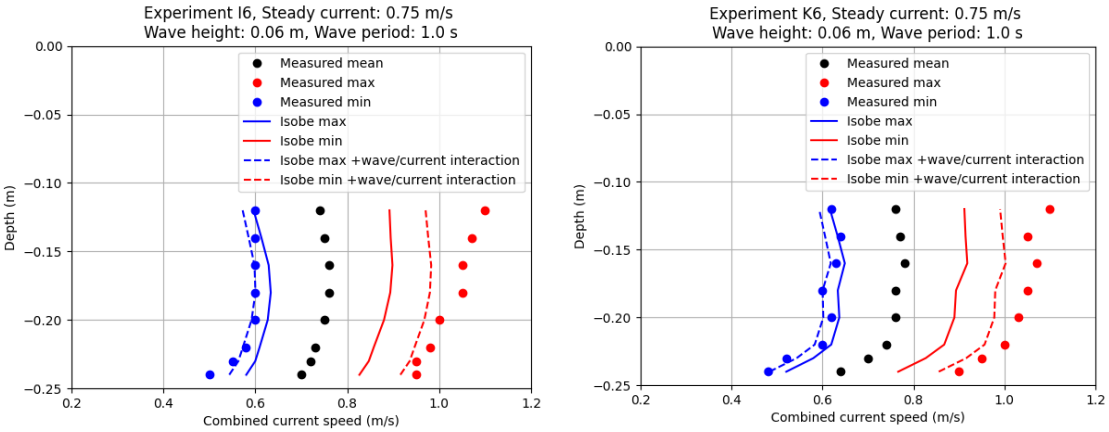

Figure 2. Measured and computed velocity profiles.

Notice, that only the nearbed wave orbital velocity is calculated with the Isobe model, meaning that the velocity variation over the depth is not captured in the figure above.

In addition, the existence of waves in the flume is expected to give rise to a return current. In some cases, the return current is estimated to be up to 5 cm/s, meaning that the actual depth-averaged velocity can be different from what it has been reported. This can also be found by calculating the depth-averaged velocity from the measurements and comparing it with the ones reported. Thus, the wave forcing needs to be adjusted to better capture the water velocity variation and the bed shear stresses.

At this stage MIKE utilizes linear wave theory to compute the nearbed wave orbital velocities and the wave orbital amplitude. This in conjunction with the discrepancies mentioned above lead to the requirement of establishing a representative wave forcing for the model. Hence, the wave height is re-calculated based on the measured nearbed velocities. More specifically, the difference between the maximum and the mean measured velocity of the three bottom points is considered and linear wave theory (applied in the bed shear stress calculation of the sediment transport model) is used to estimate the adjusted wave height. Table 1 presents the adjusted wave height for all the analyzed experiments.

A constant wave field is utilized as forcing for both the HD and MT modules according to the adjusted wave conditions for the specific run. The wave forcing is warmed up during 15 minutes.

Sediment Assumptions

The model represents the sediment grain size distribution by two fractions. One fraction corresponds to the sand fraction (d_{50}=0.13 mm) content of the bed. The other fraction corresponds to the mud (< 63 μm) content of the bed.

The fall velocity (w_s) of the mud fraction is assumed to be independent of sediment concentration and does not account for flocculation. The fall velocity is calculated using Stokes law. A relative sediment density (s) of 2.65 is assumed along with a kinematic water viscosity (v) of 10^{-6} m^2/s. The acceleration of gravity (g) is set to 9.81 m/s^2. A sediment diameter (d) of 5 μm was utilized to set the fines fraction fall velocity (w_s) equal to $2x10^{-5}$ m/s.

Bed Description

The modelled bed presents one layer with initial thickness of 5 cm (such as the laboratory flume). The initial fractions composition varies according to the analyzed experiment. The bed roughness in the MT module is set to 2.5 x d_{50} (0.000325 m) – according to the sand grain size. The bed density corresponds to the dry density of the analyzed samples mixtures – presented in Table 2.

Erosion

The bed is modelled as soft mud. The critical shear stress (τ_{ce}) is defined according to the mud content in the bed – described in section number. The power of erosion (α) and erosion coefficient (E_0) have been calibrated in order to match the simulated and measured suspended sediment concentration. Each experiment (bed) presents a unique combination of α and E_0 values for all hydrodynamics conditions. Table 5 shows the calibrated erosion parameters.

Table 5. Bed erosion parameters for the mud fraction.

Experiment	Fines content [%]	Critical shear stress (τ_{ce}) [N/m^2]	Power of erosion (α) [-]	Erosion coefficient (E_0) [kg/m^2/s]
J	13	0.125	4	1.5×10^{-4}
I	18	0.180	4	9.0×10^{-5}
K	30	0.270	4	3.5×10^{-5}

MODELLING RESULTS

Hydrodynamics

The instantaneous modelled u-velocity profile is directly compared to the observed time-averaged current velocity along the laboratory experiment duration. Additionally, the estimated wave orbital velocity profiles in onshore and offshore directions are directly compared to the maximum (crest) and minimum (trough) observed current velocity, respectively. The modelled and measured values are computed at the centre of the experiment flume for different depths. The simulated profiles correspond to the instantaneous conditions right after the warm-up period (15 minutes).

Figure 3 shows the comparison between the simulated u-velocity profiles and the measurements. In terms of time-averaged current velocity, runs 3 and 4 show a good agreement between the modelled and measured u-velocity profiles for all the experiments. Run 5 shows a slight disagreement for some specific depths over the water column. However, it still provides a good match at the bottom of the channel. A good agreement at the bottom is important for the bed shear stress calculations, which directly influences the bed erosion. Run 6 presents the most relevant disagreement when compared to the other hydrodynamic conditions. A reasonable agreement is observed at the bottom for experiments J and K. Overall, the HD model performs better for lower velocities.

The modelled hydrodynamics conditions are consistent with the experimental flume. The simulated HD volumes are utilized for the sediment calculations.

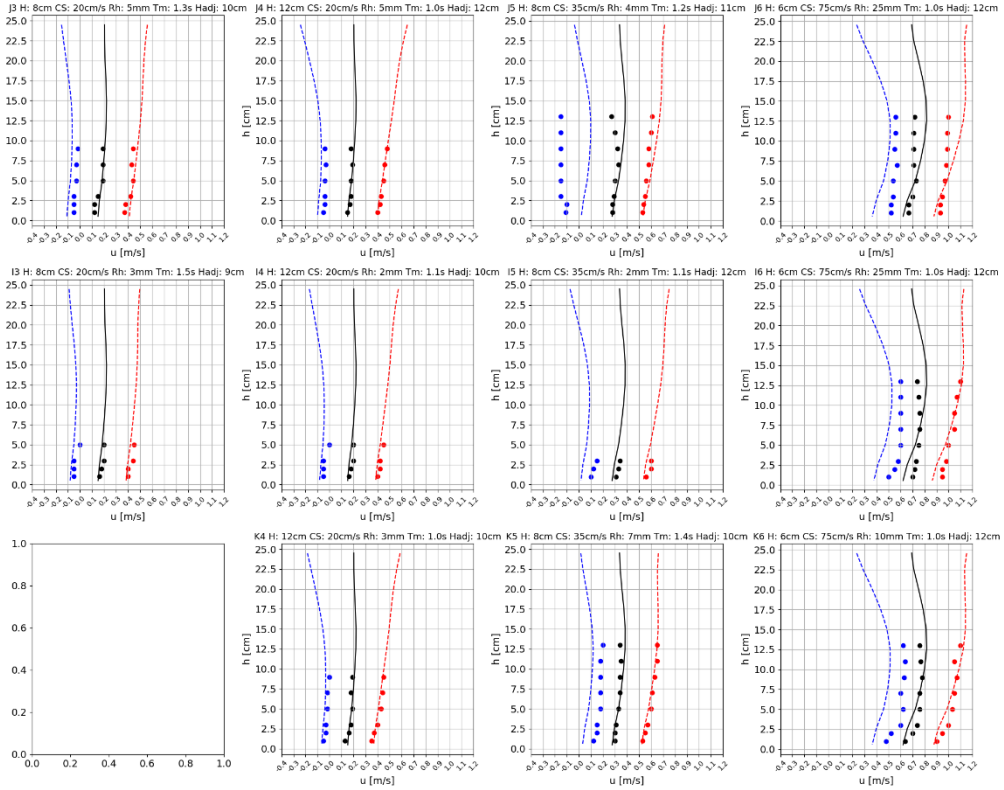

Figure 3. Current velocity profiles for experiment J, I, and K (simulated x measurements).

Sediment transport

Firstly, the modelled bed shear stresses for each experiment are presented. The simulated suspended sediment concentrations are validated with respect to the measured suspended sediment concentration during the laboratory experiments – for both fractions (i.e. sand and fines). Such as for the hydrodynamics conditions, the simulated suspended sediment concentration profiles are extracted at the middle of the model domain. The profiles correspond to the instantaneous conditions right after the warm-up period.

Bed shear stress

The modelled bed shear stress follows the (Soulsby, et al. 1993) RMS formulation for combined wave-current action. The current contribution utilizes the simulated current, while the wave contribution is directly related to the wave forcing (i.e. adjusted wave height (H_{adj}) and wave period (T)) The bed shear stress values are extracted in the middle of the model domain. It corresponds to the instantaneous conditions right after the warm-up period (15 minutes). Table 6 shows the modelled bed shear stresses for experiment I, J, an K.

Table 6. Modelled bed shear stresses for experiments I, J, and K

Run	Depth-averaged current velocity (CS) [m/s]	Wave height (H) [m]	Wave period (T) [s]	Adjusted wave height (H_{adj}) [m]	Bed shear stress (τ) [N/m^2]
J3	0.20	0.08	1.30	0.10	0.41
J4	0.20	0.12	1.00	0.12	0.45
J5	0.35	0.08	1.20	0.11	0.56
J6	0.75	0.06	1.00	0.12	1.37
I3	0.20	0.08	1.50	0.09	0.36
I4	0.20	0.12	1.10	0.10	0.38
I5	0.35	0.08	1.10	0.12	0.59
I6	0.75	0.06	1.00	0.12	1.37
K4	0.20	0.12	1.00	0.10	0.35
K5	0.35	0.08	1.40	0.10	0.52
K6	0.75	0.06	1.00	0.12	1.37

Sand fraction

Figure **4** presents the simulated and measured suspended sand concentrations at the measurement points along the water column for experiments I, J, and K over the different hydrodynamics conditions.

The plot shows that the majority of the simulated concentrations differ from the corresponding observed values by a maximum factor of 5. It is observed a significant agreement for runs J5 and K5. However, the observed concentrations in the flume for run I5 are too low and thus this case is understood as an outlier.

It is noted that the model does not match the near-bed concentration for runs J3 and I3, but a good match is reached in runs J4 and I4. The observed near-bed concentration for run number 3 is higher than in run 4 even though both runs present the same depth-averaged current velocity, and run 4 presents a higher wave. It seems that the model is either not able to capture the effect of the wave period for the bed shear stress calculations or the ripple shapes directly influence the comparison between these cases.

The model overestimates the simulated concentrations for run K6, it follows the 2-factor line. A much larger bed shear stress is estimated for run 6 when compared to the other runs due to the hydrodynamics and wave conditions. These more extreme conditions lead to much higher sediment concentrations observed in the flume. The model is able to represent this behavior, but not at the same rate of change as the observations in the flume.

Scatters exist for the sand fraction in this mixed bed results – mainly for the less extreme hydrodynamics conditions. Overall, the results are reasonable.

The measured sediment concentrations for runs I6 and J6 show a not expected profile for suspended sediment concentration across the water column – concentration gets higher close to the surface. In this sense,

Figure **4** (bottom) shows the modelled and observed depth-averaged sediment concentration in the water column. It is possible to observe that depth-average simulated values for runs I6 and J6 show a good agreement in terms of mean values in the water column.

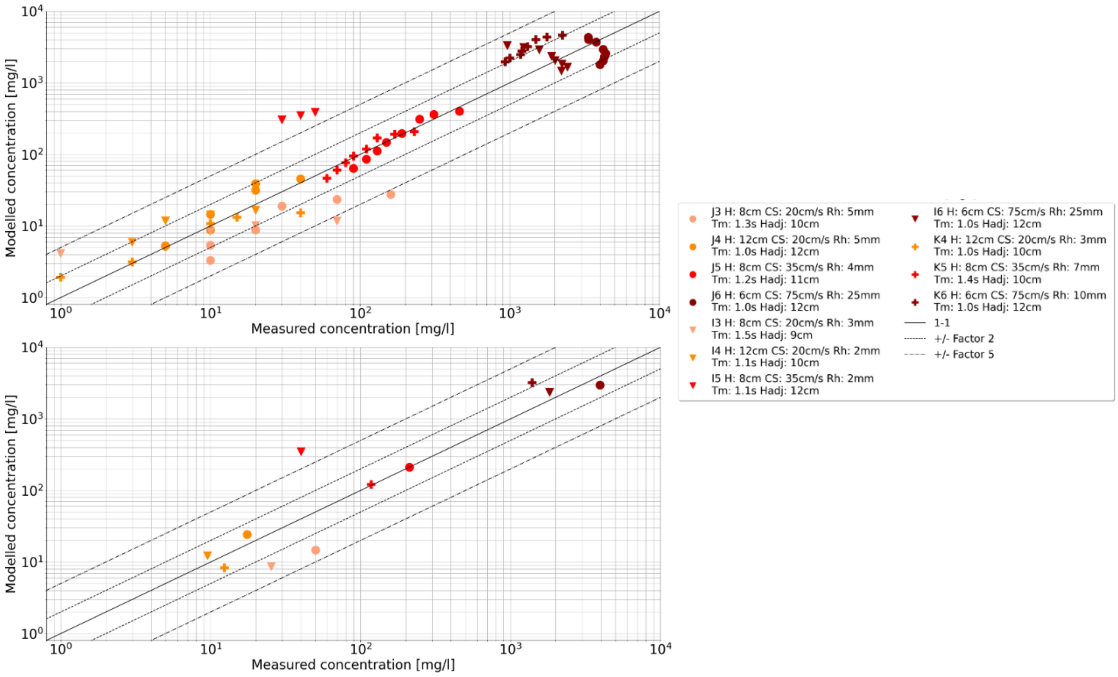

Figure 4. 1:1 representation of measured and modelled suspended sand concentration for experiments I, J, and K.

Mud fraction

Figure **5** (top) presents the simulated and measured suspended fines concentrations at the measurement points along the water column for experiments I, J, and K over different hydrodynamics conditions.

The plot suggests that most of the simulated suspended sediment concentration values differ from the measurements by a maximum factor of two.

It can also be observed, that run 6 (dark red markers) does not follow a linear pattern for any of the experiments. This is mainly due to the measured profiles that do not present an expected shape for suspended sediment concentration. Nevertheless, all the points are located in the factor 2 and 5 area. It suggests at least a certain level of agreement in terms of order of magnitude, which is clear in the depth-averaged comparison in Figure 5 (bottom).

The upper water column simulated values for experiment K4 (orange plus markers) differ from the observations by a factor larger than 2. This is mainly due to the constant suspended sediment concentration profile observed in the flume – which is not reasonable for natural conditions. Likewise, for the sand fraction, the observed profile for run I5 shows a certain level of inconsistency. The shallowest suspended concentration is understood as an outlier, and thus not utilized for the depth-averaged calculations.

Figure **5** (bottom) shows the modelled and observed depth-averaged sediment concentration in the water column. It is evident that all the points are located in the 2-factor area – or slightly close to it. Therefore, a better agreement between the model and the observations is noted when analyzing the mean values in the water column – which smooths measured outliers/non-sense profiles.

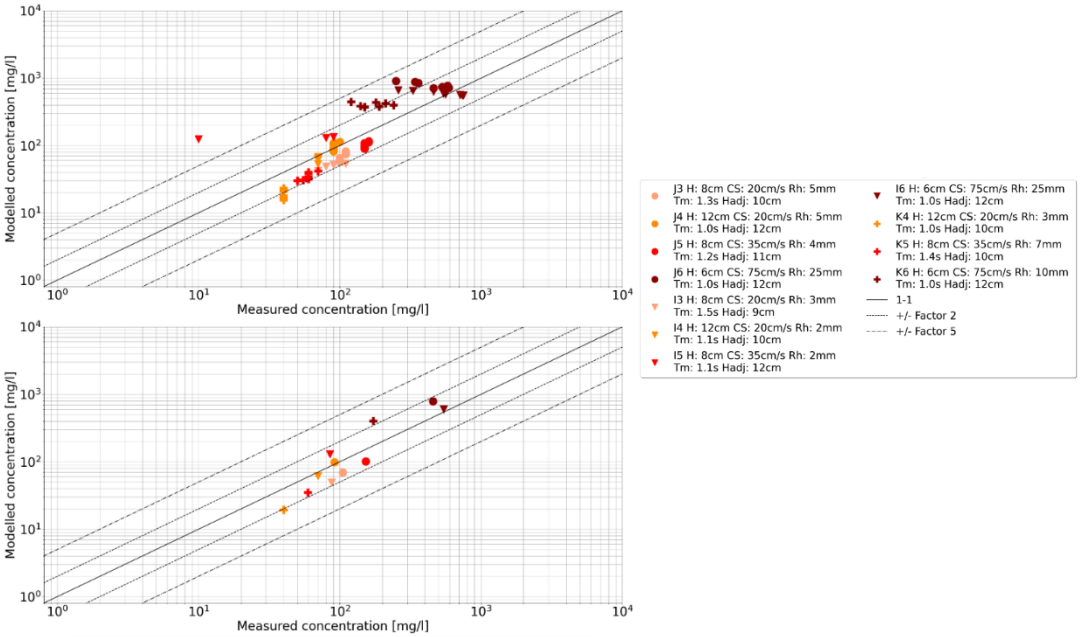

Figure 5 1:1 representation of measured and modelled suspended mud concentration for experiments I, J, and K.

DISCUSSION

The wave-current flume experiments of phase 1D (long-bed) of MUSA project were reproduced in a digital flume. The 3-D model is established in MIKE 3 Flow Model FM. The hydrodynamics module (HD) simulates the hydrodynamics volumes. The mud transport module (MT) calculates the sediment dynamics in the flume. The existing MT module – with specific improvements – models the mud fraction of the bed. While the sand fraction dynamics is calculated with a new model implementation.

The analyzed experiments cover different bed compositions. Experiments I, J, and K vary the mud content in the bed from 13% to 30%. The experiments are conducted under different hydrodynamic and wave conditions.

The hydrodynamics validation in terms of simulated u-velocity profiles indicates that the model is able to represent the current speed of the laboratory conditions. Thus, it is reasonable to utilize the HD outputs for further MT calculations.

Additionally, the measured wave orbital velocities measured in the MUSA experiments was assessed. At this stage, MIKE utilizes linear wave theory to compute the near-bed wave orbital velocity, which is utilized for calculating the bed shear stress. Due to the current-wave interaction in the flume, the wave height had to be modified in the model in order to obtain a good match between the measured wave orbital velocities and the wave orbital velocities used in the sediment transport model (which uses linear wave theory without interaction with the mean current). It is noted that in field conditions, the effect of the currents on the wave orbital motions is normally limited and the linear wave approximation is generally valid. This is the reason we did not change the calculation procedure in the model to include the effects observed in the experimental flume.

For experiments I, J, and K, model predictions for the concentration of sand and mud fractions over the water column are compared with the measurements. Generally, this comparison is within a factor of 2-5 for the sand and mud fraction.

Overall, the model performance is similar to results from the literature with respect to the comparison with this type of measurements.

Finally, the model is able to represent the observed pattern for the erosion rate over the different mud content in the bed; in which the erosion rate erosion rate decreases for higher mud content beds. Likewise for the sand fraction, the new combined mud and sand transport model is able to represent the dynamics of the fines in a sand-mud mixed bed.

REFERENCES

DHI A/S. 2021. "MIKE 21 & MIKE 3 Flow Model FM - Mud Transport Module Scientific Documentation."

DHI A/S. 2022. *MIKE 3 Flow Model FM. Hydrdynamic and Transport module. Scientific Documentation.* Horsholm: DHI A/S.

Fredsøe, J. 1984. "Turbulent boundary layer in wave-current motion." *J Hydr Eng, A S C E, Vol 110, HY8* 1103-1120.

Lenssinck, Lidian, and Anne Ton. 2024. *DEL112 - MUSA.* 01 26. https://publicwiki.deltares.nl/display/TKIP/DEL112+-+MUSA.

Parchure, T. M., and A. J. Metha. 1985. "Erosion of soft cohesive sediment deposits." *Journal of Hydraulic Engineering - ASCE 111 (10)* 1308-1326.

Shields, A. 1936. "Anwendung der Aehnlichkeitsmechanik und der Turbulenzforschung auf die Geschiebebewegung." *Mitteilungen der Preußischen Versuchsanstalt für Wasserbau und Schiffbau.*

Soulsby, R. L., L. Hamm, G. Klopman, D. Myrhaug, R. R. Simonns, and G.P. Thomas. 1993. "Wave current interaction within and outside the bottom boundary layer." *Coastal Engineering, 21* 41-69.

Wu, Weiming, and Qianru Lin. 2014. "Nonuniform sediment transport under non-breaking waves and currents." *Coastal Engineering 90* 1-11.

Wu, Weiming, Chamil Perera, Jarrel Smith, and Alejandro Sanchez. 2017. "Critical shear stress for erosion of sand and mud." *Journal of Hydraulic Research, 56:1* 96-110.

Wu, Weiming, Sam S. Y. Wang, and YAFEI JIA. 2000. "Nonuniform sediment transport in alluvial rivers." *Journal of Hydraulic Research, 38:6* 427-434.